HIGH ORDER WEIGHTED COMPACT BOUNDARY CONDITION

by

ZHENGJIE WANG

Presented to the Faculty of the Graduate School of

The University of Texas at Arlington in Partial Fulfillment

of the Requirements

for the Degree of

MASTER OF SCIENCE IN MATHEMATICS

THE UNIVERSITY OF TEXAS AT ARLINGTON

August 2008

ACKNOWLEDGEMENTS

Firstly I acknowledge my supervising advisor Dr. Chaoqun Liu, who gave me persistent support and encourage throughout my entire research activity. Without his support and motivation I would not be able to finish this thesis. Secondly I want to appreciate Ping Lu, who was working on the same project, and providing me the basic thoughts. Next, I want to thank Maria Oliveira who gave me a lot of specific suggestion throughout my graduate studies. This paper is mostly an extension research of Dr. Liu's former master student Amith Madhav Kalaghatagi, whose master thesis is initial research of the boundary algorithm for Weighted Compact Scheme. And I reference several introduction paragraphs from his thesis. But the most difference between our works is that I gave back the original taste of WCS to WCS at boundaries' nodes. And this difference, he mentioned in Chapter 5, future work, of his thesis, even though he did not know who would take over this job. Anyway, I acknowledge him for his initial work and thesis.

Finally I would like to thank my family and friends who have been giving me constant inspiration and moral support. I would particularly like to thank my friends Ms. Li Liu, Mr. Cen Wu.

July 29, 2008

ABSTRACT

HIGH ORDER WEIGHTED COMPACT BOUNDARY CONDITION

Zhengjie Wang, M.S.

The University of Texas at Arlington, 2008

Supervising Professor: Chaoqun Liu

Committee Members: Hristo Kojouharov, Jianzhong Su

Key words: Numerical Computation, Derivatives, Weighted Compact Scheme, Boundary

In multi-dimension flows, we expect to have problems at the boundaries when a shock hits or reflects at the boundary wall the remedy to this would be to develop weighted boundary conditions similar to the Weighted Compact Scheme for the interior nodes, by choosing candidate stencils around the boundary nodes and assigning weights to each of these stencils with the ENO reconstruction. This would avoid spurious oscillations when shocks are encountered at the boundaries.

This thesis investigates higher order weighted compact boundary conditions for Weighted Compact Scheme (WCS). WCS is a combination of Essentially Non Oscillatory Scheme and Weighted Compact Finite Difference Schemes with Spectral-like Resolution. Implicit higher order schemes for spatial derivatives are derived for nodes in the neighborhood of the boundaries for the existing WCS scheme, which is used for the interior nodes. The objective is to achieve a higher weighted algorithm at the boundary, by using a compact stencil. To obtain this target, a combination of the spatial nodes' derivatives and values is going to be used.

Several higher order schemes for the boundaries are derived and tested for both sine function and exponential function under 1st, 2nd and 3rd Boundary Condition. This new boundary scheme not only preserves the characteristic of standard compact schemes and achieves high order accuracy and high resolution using compact stencils, but also has the potential ability to accurately capture shock waves and discontinuities without oscillation. Numerical examples show the scheme is very promising and successful.

TABLE OF CONTENTS

LIST OF FIGURES

Figure

LIST OF TABLES

Table

CHAPTER 1

INTRODUCTION

1.1 Review and development of Higher Order Scheme

Considerable progress has been made over the past two decades on developing high-order accuracy and high-resolution schemes for calculating flow fields with shocks. In the simulation of complex flow fields containing shock waves, most efforts have been paid to the shock-capturing method. It is well known that first-order accurate schemes are too diffusive, but classical central high-order schemes exhibit spurious oscillations around such nodes. In order to capture shock waves smoothly without spurious oscillations, the development of non-oscillatory dissipative schemes containing no free parameters with high resolution has much been emphasized just recent [7].

On the other hand, many physical phenomena possess a wide range of length and time scales, turbulent fluid flows being a common example. Direct numerical simulations of these processes require all the relevant scales to be properly represented in the numerical model. Due to the above reasons, the accuracy requirement in the large-eddy simulations and direct numerical simulations of turbulence, computational electromagnetic and computational aero acoustics has become a pacing item for technology development [7].

High order finite difference schemes are based on interpolations of discrete data, mostly by using algebraic polynomials. Traditional finite difference schemes are based on fixed stencil interpolations. For example, to obtain an interpolation for cell i to third order accuracy, the information of the three cell i-1, i and i+1 are used to build second order interpolation polynomial. This works well for globally smooth problems. The resulting scheme is linear for linear PDEs, hence stability can be analyzed by Fourier transforms (for the uniform grid periodic case). However, fixed stencil interpolation of second or higher order accuracy is certainly

oscillatory near discontinuities. Such oscillations, which are called Gibbs phenomena in spectral methods, do not decay in magnitude when the mesh is refines. It is a nuisance to say the least for practical computation, and often leads to numerical instabilities in nonlinear problems containing discontinuities [7].

Earlier attempts to eliminate or reduce such spurious oscillations near discontinuities were mainly based on two approaches: explicit artificial viscosity and limiters. The first approach was to add artificial viscosity which could be tuned so that it was large enough near the discontinuity to suppress, or at least reduce the oscillations, but was small elsewhere to maintain high-order accuracy. One disadvantage of this approach is that delicate tuning of the parameters controlling the artificial viscosity is problem dependent. The second approach was to apply limiters to eliminate the oscillations. In effect, one reduced the order of accuracy of the interpolation near the discontinuities [7].

ENO (Essentially Non-Oscillatory) schemes first introduced by Harten, Engquist, Osher and Chakravarthy [2], were the first attempt to obtain uniformly high order accurate, yet essential non-oscillatory interpolation for piecewise smooth functions. The reconstruction in [2] is a natural extension of an earlier second order version of Harten and Osher [12]. The ENO schemes choose the smoothest stencil to pick on interpolating polynomial for the ENO reconstruction [7].

Later Weighted ENO (WENO) schemes were developed, using a convex combination of all candidate stencils instead of just one as in the original ENO [4]. WENO schemes remove all the stencils choosing procedures in ENO which is very time consuming. In WENO each of the candidate stencils is assigned a weight that determines the construction of the stencil to the final approximation of the numerical flux [5]. The weighted are defined in such a way that in smooth regions it approaches certain optimal weights to achieve a higher order of accuracy, while in regions near discontinuities; the stencils that contains the discontinuity are assigned a nearly zero weight [7].

Recently compact schemes have been widely used in the simulation of complex flows, especially in the direct numerical simulation of turbulent flows [6]. Standard finite difference schemes have explicit forms and need to be at least one point wider than the desired approximation order. Compared to standard finite difference approximations, the compact schemes can achieve higher order without increasing stencil width. As compact schemes have implicit forms and involve derivative values of neighboring grid nodes, additional free parameters can be used not only to improve the accuracy but also to optimize the other properties such as resolution and stability. The resolution characteristics mean the accuracy with which the difference approximation represents the exact result over the full range of length scales that can be realized on a given mesh. The notion of resolution is quantified by means of a Fourier analysis of the differencing scheme, and is the largest wave number that can be accurately represented by the scheme. The resolution characteristic of the scheme is essentially important in complex flow simulations. A family of centered compact schemes proposed by Lele has been proved to have spectral like resolution [3]. Thought the advantages of compact schemes are obvious, there are still difficulties in using them to solve problems involving shock waves or discontinuities. When they are used to differentiate a discontinuous function, the computed derivative has grid to grid oscillation. Compact schemes for filtering are always used together with Compact Schemes for derivative to eliminate numerical oscillations [3], but even filtering can not reduce oscillations near discontinuities. Adams [13] proposed the hybrid compact-ENO scheme for shock-turbulence interaction problems, in which the upwind-biased compact schemes are coupled with ENO schemes. A detection algorithm is used to identify cells containing the large gradients, and then the flux derivative at the faces of such cells is computed with ENO schemes. In this approach, the detection procedure is very time consuming [7].

In [1] a new class of compact schemes called the Weighted Compact Schemes (WCS) was developed. WCS is a hybrid of different forms of standard schemes. WCS uses the idea of

WENO and the Compact Finite Difference Schemes and hence the name WCS. WCS uses a set of candidate stencils, and on each candidate stencil, for a given order of accuracy, there is a corresponding finite difference compact scheme. According to the smoothness of each stencil, a weight is assigned to each finite difference approximation obtained by compact scheme. The weights are defined in such a way that the stencils, including the discontinuities, have less contribution to the final scheme. Thus, the non-oscillatory property is achieved near discontinuities, while high order accuracy and high resolution properties of compact schemes can still be preserved in the smooth region. Another problem while using compact scheme is the conservation property of the scheme. Conservation property is especially important in solving problems involving shocks. Non-conservative methods usually generate large errors near the shock [5]. Using the primitive function reconstruction method of ENO scheme to a compact scheme can maintain the conservation property, and this is the method applied in WCS to achieve conservation [7].

In this paper, weighted high order compact schemes are developed for the nodes in the neighborhood under 1st, 2nd and 3rd boundary conditions. This paper is organized as follows; Chapter 2 discusses the derivation of the Weighted Compact Scheme in detail. Derivation of schemes for the boundary nodes are discussed in Chapter 3. The Weighted Compact Scheme with the derived boundary nodes are represented in Chapter 3. The Weighted Compact Boundary under all the 3 kinds' boundary conditions is implemented for various functions, which is discussed in Chapter 4. Conclusion and future work for this scheme is discussed in Chapter 5.

CHAPTER 2

WEIGHTED COMPACT SCHEME

2.1 Basic Formula of Weighted Compact Scheme

Given the function values on a set of nodes, the finite difference approximation to the derivative of the function is expressed as a linear combination of the given function value. For simplicity, consider a uniform spaced mesh where the nodes are indexed by *j*. The independent variable at the node *j* is $x_j = h(j\text{-}1)$ for $1 \le j \le N$ and the function values at the nodes $f_j = f(x_j)$ are given. The finite difference approximation f_j' to the first derivative at the node *j* can be written in the following general form by using the finite difference compact scheme [3] (Lele, 1992),

$$\beta_- f_{j-2}' + \alpha_- f_{j-1}' + f_j' + \alpha_+ f_{j+1}' + \beta_+ f_{j+2}' = \frac{1}{h}(b_- f_{j-2} + a_- f_{j-1} + f_j + a_+ f_{j+1} + b_+ f_{j+2}) \tag{2.1}$$

For a given node *j*, three candidate stencils containing this node are defined as follows:

$S_0 = (x_{j-2}, x_{j-1}, x_j)$, $S_1 = (x_{j-1}, x_j, x_{j+1})$, $S_2 = (x_j, x_{j+1}, x_{j+2})$

Interior Stenciles

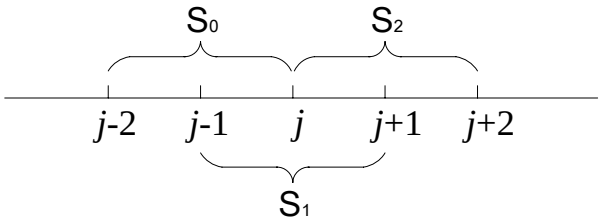

Figure 2.1 Candidate Stencils for an interior node j

On each stencil a finite difference compact scheme is derived in the form of equation (2.1) by matching the Taylor series coefficients to various orders. The coefficients for the three stencils are given in Table 1.1.

Table 1.1 Coefficients for the candidate stencils S_0, S_1 and S_2

	β_-	α_-	α_+	β_+	b_-	a_-	c	a_+	b_+
S_0	θ	$2\theta+2$	0	0	$-5\theta/2-1/2$	$2\theta-2$	$\theta/2+5/2$	0	0
S_1	0	1/4	1/4	0	0	-3/4	0	3/4	0
S_2	0	0	$2\theta+2$	θ	0	0	$-\theta/2-5/2$	$-2\theta+2$	$5\theta/2+1/2$

where θ is a free parameter. θ is set to zero to get a tridiagonal matrix. This parameter can also be used to improve the accuracy or optimize the scheme. The sacrifice would be to increase the computer time.

The schemes for the three candidate stencils are got by applying equation (2.1) to each of these stencils and are given by equation (2.2).

S_0: F_0 $$2f_{j-1}'+f_j'=\frac{1}{h}(-\frac{1}{2}f_{j-2}-2f_{j-1}+\frac{5}{2}f_j)$$

S_1: F_1 $$\frac{1}{4}f_{j-1}'+f_j'+\frac{1}{4}f_{j+1}'=\frac{1}{h}(-\frac{3}{4}f_{j-1}+\frac{3}{4}f_{j+1})$$

S_2: F_2 $$f_j'+2f_{j+1}'=\frac{1}{h}(-\frac{5}{2}f_j+2f_{j+1}+\frac{1}{2}f_{j+2}) \quad (2.2)$$

The schemes corresponding to stencils S_0 and S_2 are third order one-sided finite difference schemes (bias difference), and the scheme corresponding to S1 is a fourth order centered scheme. These three equations are denoted by F_0, F_1 and F_2. Then a specific weight is assigned to each equation, and a new scheme is obtained by a summation of the equations.

$$F=C_0F_0+C_1F_1+C_2F_2 \quad (2.3)$$

Where, C_0, C_1, and C_2 are weights and satisfy $C_0 + C_1 + C_2 = 1$. If the weights are properly chosen, the scheme achieves a higher order of accuracy because the additional free parameters are introduced. If the coefficients are chosen as

$$C_0 = C_2 = \frac{1}{18 - 24\theta},\ C_1 = \frac{8 - 12\theta}{9 - 12\theta} \tag{2.4}$$

Then the new scheme obtained by setting θ to zero is a sixth order centered compact scheme and is given by:

$$\frac{1}{3} f_{j-1}' + f_j' + \frac{1}{3} f_{j+1}' = \frac{1}{h}(-\frac{1}{36} f_{j-2} - \frac{7}{9} f_{j-1} + \frac{7}{9} f_{j+1} + \frac{1}{36} f_{j+2}) \tag{2.5}$$

The procedure described above implies that a sixth order centered compact scheme can be represented by a combination of three lower order schemes.

The scheme (2.5) is a standard finite difference compact scheme and cannot avoid the oscillations near discontinuities. In order to achieve non-oscillatory property, the method of the WENO scheme [2] (Jiang et al. 1996) is introduced to determine the new weight for each stencil. The weights are determined according to the smoothness of the function on each stencil. Following the WENO method, the new weights are defined as

$$\omega_k = \frac{\gamma_k}{\sum_{i=0}^{2} \gamma_i} \qquad \gamma_k = \frac{C_k}{(\varepsilon + IS_k)^P} \qquad k = 0,1,2 \tag{2.6}$$

Where, ε is a small positive number which is used to prevent the denominator becoming zero, P is important parameter to control weight. IS_k is the smoothness measurement which is defined according to WENO [5],

$$IS_0 = \frac{13}{12}(f_{j-2} - 2f_{j-1} + f_j)^2 + \frac{1}{4}(f_{j-2} - 4f_{j-1} + 3f_j)^2$$

$$IS_1 = \frac{13}{12}(f_{j-1} - 2f_j + f_{j+1})^2 + \frac{1}{4}(f_{j-1} - f_{j+1})^2$$

$$IS_2 = \frac{13}{12}(f_j - 2f_{j+1} + f_{j+2})^2 + \frac{1}{4}(3f_j - 4f_{j+1} + f_{j+2})^2 \tag{2.7}$$

Where, the two terms on the right side can be regarded as the measurements of the curvature and the slope respectively at a certain point. Through the Taylor expansion, it can be easily proved that in smooth regions new weights ω_k satisfy:

$$\omega_k = C_k + O(h^2) \text{ and } \omega_2 - \omega_0 = O(h^3) \tag{2.8}$$

The new scheme is formed using these new weights:

$$F = \omega_0 F_0 + \omega_1 F_1 + \omega_2 F_2 \tag{2.9}$$

The leading error of F is a combination of the leading errors of the original schemes, which is:

$$(\frac{1}{12}\omega_0 - \frac{1}{12}\omega_2) f^{(4)} h^3 + (-\frac{1}{15}\omega_0 + \frac{1}{120}\omega_1 - \frac{1}{15}\omega_2) f^{(5)} h^4 \tag{2.10}$$

When equation (2.9) is satisfied, the leading error of the new scheme can be written as $O(h^6)$. This scheme is of sixth-order accuracy and has the high resolution property as the centered sixth-order compact scheme in smooth regions. But in the regions containing discontinuities, the smoothness measurement IS_k of the non-smooth stencil is large compared to that of the smooth stencil, thus the non-smooth stencil is assigned a small weight and has less contribution to the final scheme so that the non-oscillatory property is achieved.

With the new weights ω_k, the new finite difference compact scheme equation (2.8) is written in the form of equation (2.1). The coefficients of the final Weighted Compact Scheme with the weights for each stencil is given as follows:

Table 1.2 Coefficients of the final Weighted Compact Scheme with weights

β_-	$\theta\omega_0$
α_-	$(2\theta+2)\ \omega_0 + \omega_1/4$
α_+	$(2\theta+2)\ \omega_2 + \omega_1/4$
β_+	$\theta\omega_2$
b_-	$(-5\theta/2-1/2)\ \omega_0$
a_-	$(2\theta-2)\ \omega_0 - 3\omega_1/4$
c	$(\theta/2+5/2)\ \omega_0 - (\theta/2+5/2)\ \omega_2$
a_+	$(-2\theta+2)\omega_2 + 3\omega_1/4$
b_+	$(5\theta/2+1/2)\ \omega_2$

As ω_k is dependent on the smoothness measurement calculated by local function values, the scheme coefficients vary from node to node. The free parameter θ can be used to optimize the scheme when the properties of high resolution and stability are concerned. If θ is set to zero, the matrix formed by the scheme is tridiagonal. Though in the above description the sixth-order Weighted Compact Scheme is selected as an example, the method can be extended to a general form [1].

2.2 Conservative formulation

The conservative property of the scheme is very important in shock wave capturing, since it imposes a constraint on the solution error. Non-conservative schemes usually generate shocks that have the wrong strength and travel at the wrong speed. In the work of Davis [8] (1998), the reconstruction method developed by Shu and Osher [9] for the ENO scheme was used together with the Pade scheme to achieve the conservation. The finite difference scheme developed itself is not conservative. However, conservation can be obtained when the weighted compact scheme is applied together with ENO reconstruction method. The method is described below. For 1-D conservation laws:

$$u_t(x,t) + f_x(u(x,t)) = 0 \tag{2.11}$$

When a conservative approximation to the spatial derivative is applied, a semi-discrete conservative form of equation (2.10) is as follows:

$$\frac{du_j}{dt} = -\frac{1}{\Delta x}(\hat{f}_{j+\frac{1}{2}} - \hat{f}_{j-\frac{1}{2}}) \tag{2.12}$$

$\hat{f}_{j+\frac{1}{2}}$ and $\hat{f}_{j-\frac{1}{2}}$ are numerical flux functions at the cell interfaces. Δx is the grid size of the uniform grid. In order to achieve the high order accuracy, the numerical flux should be defined in such a way that the difference of the numerical flux is a high order approximation of the derivative f_x. According to the ENO reconstruction procedure [12], it has been approved that the

primitive function of $\hat{f}$ at the cell interfaces can be exactly calculated by the given node values f_j. If H is the primitive function of $\hat{f}$, then:

$$H(x_{j+\frac{1}{2}}) = \Delta x \sum_{i=-\infty}^{j} f_i \tag{2.13}$$

The numerical flux $\hat{f}$ at the cell interfaces is the derivative of its primitive function H i.e.:

$$\hat{f}_{j+\frac{1}{2}} = H'_{j+\frac{1}{2}} \tag{2.14}$$

As the values of the function H have already been obtained at the cell interfaces, the approximations of the derivatives of H at the cell interfaces are calculated directly by the Weighted Compact Scheme presented in Section 2.1. Thus, the WCS are applied to the primitive function instead of the function itself. In this way the conservation property is achieved.

CHAPTER 3

WEIGHTED COMPACT BOUNDARY CONDITIONS FOR WCS

Interior nodes use a five nodes stencil, i.e. , at an interior node j, to compute the first derivative we use two nodes to the left and two nodes to the right, which gives us a centered scheme in smooth regions. But when we approach the neighborhood of the boundary, like nodes 1, 2, we do not have two nodes on the left; neither have we had two nodes on the right side of node N-1, N. So we have to derive high order compact schemes which is different from the interior stencils' scheme at these boundary nodes. Node 1, N and 2, N-1 use the same scheme, except the coefficients have a different sign on the right hand side of the equation which we will see after they are derived. So basically we need to derive two weighted compact schemes at nodes 1 and 2.

Also another issue for the global accuracy of a scheme is that it is partially dependent on the accuracy of the boundary conditions. It has been observed that in order to have a high order of accuracy globally, it is not sufficient if we have a higher order at the interior but also we need to have a higher order equally at the boundaries. It has been confirmed that the highest global accuracy achievable is on order higher than that of the boundary, for example if we need a sixth order accuracy globally than the boundary should be at least fifth order accurate. Also one of the problems is the numerical instabilities due to the boundary conditions, which if left unchecked these spurious waves amplify and eventually wipe out the entire solution. Hence the objective of this paper is to achieve such a higher order accurate and weighted compact scheme that the neighborhood of boundary nodes.

3.1 Boundary Node 1 in First Boundary Condition

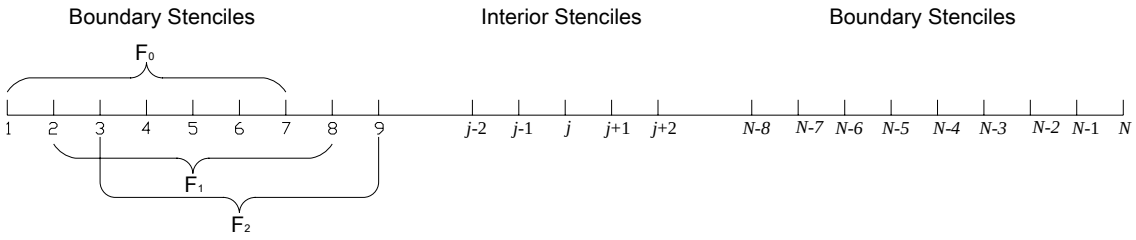

Figure 3.1 Stencils at Boundary nodes 1

At boundary node 1 the neighboring nodes lie on left side. In this case the form the compact scheme is:

F_0 :

$$f_1'+6f_2' = \frac{1}{h}\left(-\frac{69}{20}f_1 - \frac{17}{10}f_2 + \frac{15}{2}f_3 - \frac{10}{3}f_4 + \frac{5}{4}f_5 - \frac{3}{10}f_6 + \frac{1}{30}f_7\right)$$

F_1 :

$$f_1' - \frac{363}{20}f_2' = \frac{1}{h}\left(\frac{13327}{400}f_2 - \frac{1299}{20}f_3 + \frac{1369}{24}f_4 - 39f_5 + \frac{285}{16}f_6 - \frac{1439}{300}f_7 + \frac{23}{40}f_8\right)$$

F_2 :

$$f_1' - \frac{1924}{363}f_2' = \frac{1}{h}\left(\frac{90743}{3630}f_3 - \frac{141353}{1815}f_4 + \frac{483139}{4356}f_5 - \frac{34348}{363}f_6 + \frac{35699}{726}f_7 - \frac{78497}{5445}f_8 + \frac{13327}{7260}f_9\right) \quad (3.1)$$

At the right hand side of the equation presented above, seven nodes' function values are used to obtain sixth-order accuracy. F_0, F_1, F_2 are all sixth-order accuracy, and this guarantee the

weighted compact scheme is at least sixth-order accuracy. The reason we abandon the previous third-order combining fourth-order scheme boundary algorithm, is that if it is compact scheme, there are just constant C_k which would not change through the entire computation. So the final scheme $F = C_0F_0 + C_1F_1 + C_2F_2$ can cancel fourth-order and fifth-order item. But in the weighted compact scheme, C_k transform to ω_k, and ω_k are keep changing in the entire computation. So the final weighted scheme $F = \omega_0F_0 + \omega_1F_1 + \omega_2F_2$ can not guarantee cancel 3rd and 4th order items. At last, make the boundary condition only 3rd order accuracy. For here, we do not keep $\omega_0 = \omega_2$ any more. Because it is boundary stencil, not interior stencil. We make $C_0 = C_1 = C_2 = 1/3$, so if the function is equally smooth at node 1, 2, 3, ω_k will have the same value. And each ω_k will contribute equally to the final weighted compact scheme. And if the function is not equally smooth at node 1, 2, 3, ω_k will be different certainly. But the final weighted compact scheme will be still six-order accurate despite of ω_k 's value. If one of the three nodes is not smooth, the scheme presented by that node will contribute very little to the final weighted compact scheme. Next session will elaborate on why $C_0 = C_1 = C_2 = 1/3$.

3.1.2 C_k and ω_k

Mathematically, we do not have to use seven nodes' function value to express the combination of f_1' and f_2' to obtain a sixth order accuracy compact scheme. For node 1, if we set, for instance,

F_0, using 5 nodes bias difference:

$$f_1' + 4f_2' = \frac{1}{h}\left(-\frac{37}{12}f_1 + \frac{2}{3}f_2 + 3f_3 - \frac{2}{3}f_4 + \frac{1}{12}f_5\right) - \frac{1}{30}f_1^{(6)}h^5 - \frac{11}{210}f_1^{(7)}h^6$$

F_1, using 6 nodes bias difference:

$$f_1' - \frac{147}{10}f_2' = \frac{1}{h}\left(\frac{4973}{200}f_2 - \frac{177}{4}f_3 + \frac{187}{6}f_4 - 16f_5 + \frac{39}{8}f_6 - \frac{197}{300}f_7\right) + \frac{69}{140}f_1^{(7)}h^6$$

F_2, using 5 nodes bias difference:

$$f_1' - \frac{522}{137} f_2' =$$
$$\frac{1}{h}\left(\frac{5589}{548} f_3 - \frac{9569}{411} f_4 + \frac{2781}{137} f_5 - \frac{1197}{137} f_6 + \frac{2501}{1644} f_7\right) - \frac{4973}{2740} f_1^{(6)} h^5 - \frac{14279}{2740} f_1^{(7)} h^6$$

And set $C_0 = \frac{207}{185}, C_1 = -\frac{18100}{184001}, C_2 = -\frac{18906}{920005}$, then $C_0 + C_1 + C_2 = 1$. And the combination $F = C_0 F_0 + C_1 F_1 + C_2 F_2$ can cancel h^5 and h^6 items. Because $-\frac{1}{30} C_0 - \frac{4973}{2740} C_2 = 0$ will cancel h^5 items, and $-\frac{11}{210} C_0 + \frac{69}{140} C_1 - \frac{14279}{2740} C_2 = 0$ will cancel h^6 items. The final scheme will obtain sixth order accuracy. But actually that is not going to happen in weighted scheme, because ω_k are different from C_k. Let's take $f(x) = \sin x$ to make a numerical explanation, we are going to use compact and weighted compact scheme deriving in this session to calculate $\cos x$. Dividing $[-\pi, \pi]$ into 40 subintervals, then $h = \pi/20$.

$$IS_0 \approx (hf_1')^2 = \left(\frac{\pi}{20}\cos 0\right)^2 = 0.0246740$$

$$IS_1 \approx (hf_2')^2 = \left(\frac{\pi}{20}\cos\frac{\pi}{20}\right)^2 = 0.0240702$$

$$IS_2 \approx (hf_2')^2 = \left(\frac{\pi}{20}\cos\frac{\pi}{20}\right)^2 = 0.0240702$$

Assuming $\varepsilon = 0.976$, $P = 1$

$$\gamma_0 = \frac{C_0}{(\varepsilon + IS_0)^P} = \frac{C_0}{(\varepsilon + IS_0)^1} = \frac{C_0}{1.0006740} = 1.1181653$$

$$\gamma_1 = \frac{C_1}{(\varepsilon + IS_1)^P} = \frac{C_1}{(\varepsilon + IS_1)^1} = \frac{C_1}{1.0000702} = -9.836213 \times 10^{-4}$$

$$\gamma_2 = \frac{C_2}{(\varepsilon + IS_2)^P} = \frac{C_2}{(\varepsilon + IS_2)^1} = \frac{C_2}{0.9983179} = -0.020584514$$

Then,

$$\omega_0 = \frac{\gamma_0}{\sum_{i=0}^{2}\gamma_i} = \frac{\gamma_0}{1.0965483947} = \frac{C_0}{1.0006740 * 1.0965483947} = 1.097287$$

$$\omega_1 = \frac{\gamma_1}{\sum_{i=0}^{2}\gamma_i} = \frac{\gamma_1}{1.0965483947} = \frac{C_1}{1.0000702 * 1.0965483947} = -8.96952896 \times 10^{-4}$$

$$\omega_2 = \frac{\gamma_2}{\sum_{i=0}^{2}\gamma_i} = \frac{\gamma_2}{1.0965483947} = \frac{C_2}{0.9983179 * 1.0965483947} = -0.01880373$$

In the final weighted compact scheme $F = \omega_0 F_0 + \omega_1 F_1 + \omega_2 F_2$ can not cancel h^5 and h^6 items. And the final scheme will at most achieve fourth order. That is reason why we make each F_k sixth-order accuracy.

3.1.3 Error Analysis

F_0:

$$f_1' + 6 f_2' - \frac{1}{h}\left(-\frac{69}{20} f_1 - \frac{17}{10} f_2 + \frac{15}{2} f_3 - \frac{10}{3} f_4 + \frac{5}{4} f_5 - \frac{3}{10} f_6 + \frac{1}{30} f_7\right) \sim -\frac{1}{56} f_1^{(8)} h^7$$

F_1:

$$f_1' - \frac{363}{20} f_2' - \frac{1}{h}\left(\frac{13327}{400} f_2 - \frac{1299}{20} f_3 + \frac{1369}{24} f_4 - 39 f_5 + \frac{285}{16} f_6 - \frac{1439}{300} f_7 + \frac{23}{40} f_8\right)$$
$$\sim -\frac{503}{1120} f_1^{(8)} h^7$$

F_2:

$$f_1' - \frac{1924}{363} f_2' - \frac{1}{h}\left(\frac{90743}{3630} f_3 - \frac{141353}{1815} f_4 + \frac{483139}{4356} f_5 - \frac{34348}{363} f_6 + \frac{35699}{726} f_7 - \frac{78497}{5445} f_8 + \frac{13327}{7260} f_9\right)$$
$$\sim -\frac{208903}{101640} f_1^{(8)} h^7$$

The combination error in the final weighted compact boundary condition will be seventh order.

3.2 Boundary Node 2 in First Boundary Condition

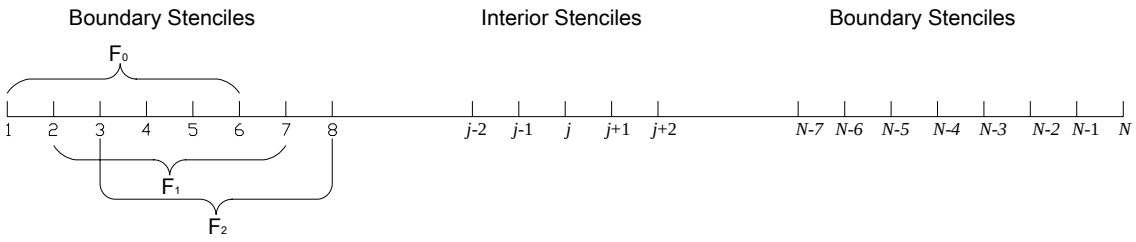

Figure 3.2 Stencils at Boundary nodes 2

The compact scheme is:

F_0:

$$\frac{1}{10} f_1' + f_2' + f_3' = \frac{1}{h}(-\frac{227}{600} f_1 - \frac{13}{12} f_2 + \frac{7}{6} f_3 + \frac{1}{3} f_4 - \frac{1}{24} f_5 + \frac{1}{300} f_6)$$

F_1:

$$-\frac{5}{177} f_1' + f_2' + \frac{345}{118} f_3' = \frac{1}{h}(-\frac{9283}{3540} f_2 + \frac{475}{472} f_3 + \frac{1085}{531} f_4 - \frac{185}{354} f_5 + \frac{25}{236} f_6 - \frac{227}{21240} f_7)$$

F_2:

$$-\frac{69}{586} f_1' + f_2' - \frac{39981}{5860} f_3' = \frac{1}{h}(\frac{1122869}{11720} f_3 - \frac{17867}{1172} f_4 + \frac{29473}{3516} f_5 - \frac{1031}{293} f_6 + \frac{4274}{4688} f_7 - \frac{9283}{87900} f_8) \quad (3.2)$$

Just as stated above, we make $C_1 = C_2 = C_3 = 1/3$, so if the function is equally smooth at node 1, 2, 3, ω_k will have the same value. And each ω_k will contribute equally to the final weighted compact scheme. And if the function is not equally smooth at node 1, 2, 3, ω_k will be different certainly. But the final weighted compact scheme will be still six-order accurate despite of ω_k 's value. If one of the three nodes is not smooth, the scheme presented by that node will contribute very little to the final weighted compact scheme.

3.2.2 Error Analysis

F_0:

$$\frac{1}{10} f_1' + f_2' + f_3' - \frac{1}{h}(-\frac{227}{600} f_1 - \frac{13}{12} f_2 + \frac{7}{6} f_3 + \frac{1}{3} f_4 - \frac{1}{24} f_5 + \frac{1}{300} f_6) \sim -\frac{1}{1680} f_2^{(8)} h^7$$

F_1:

$$-\frac{5}{177} f_1' + f_2' + \frac{345}{118} f_3' - \frac{1}{h}(-\frac{9283}{3540} f_2 + \frac{475}{472} f_3 + \frac{1085}{531} f_4 - \frac{185}{354} f_5 + \frac{25}{236} f_6 - \frac{227}{21240} f_7)$$
$$\sim \frac{79}{19824} f_2^{(8)} h^7$$

F_2:

$$-\frac{69}{586} f_1' + f_2' - \frac{39981}{5860} f_3' - \frac{1}{h}(\frac{1122869}{11720} f_3 - \frac{17867}{1172} f_4 + \frac{29473}{3516} f_5 - \frac{1031}{293} f_6 + \frac{4274}{4688} f_7 - \frac{9283}{87900} f_8)$$
$$\sim \frac{3431}{46880} f_2^{(8)} h^7$$

The combination error in the final weighted compact scheme will be seventh order.

3.3 Boundary Node 1 in Second & Third Boundary Condition

Under the First Boundary Condition, all *f* are all known. But under Second Boundary Condition, f_1' is known other than f_1. Under the Third Boundary Condition, what we know is just $a \cdot f_1 + b \cdot f_1' = c$. We can merge Second Boundary Condition into Third Boundary Condition with assuming $a = 0$ and $b = 1$. With the same bias difference method, another combination of f_1 and f_1' can be represented by

F_0 :

$$f_1 + \frac{140}{363} f_1' = \frac{1}{h}(\frac{980}{363} f_2 - \frac{490}{121} f_3 + \frac{4900}{1089} f_4 - \frac{1225}{363} f_5 + \frac{196}{121} f_6 - \frac{490}{1089} f_7 + \frac{20}{363} f_8)$$

Making it compact,

F_1 :

$$f_1 + \frac{280}{481} f_1' = \frac{1}{h}\left(\frac{3920}{481} f_3 - \frac{31360}{1443} f_4 + \frac{14700}{481} f_5 - \frac{12544}{481} f_6 + \frac{19600}{1443} f_7 - \frac{1920}{481} f_8 + \frac{245}{481} f_9\right) \quad (3.3)$$

And then define C_k and ω_k to make the scheme weighted,

$$C_0 = C_1 = \frac{1}{2}, \qquad \gamma_k = \frac{C_k}{(\varepsilon + IS_k)^P} \qquad \omega_k = \frac{\gamma_k}{\sum_{i=0}^{2} \gamma_i}$$

$$k = 0,1$$

Weighted Compact Scheme: $F = \omega_0 F_0 + \omega_1 F_1$ (3.4)

Then F combines the Third Boundary Condition $a \cdot f_1 + b \cdot f_1' = c$, forming a linear system.

Solving this linear system, we can get f_1 and f_1'. So in main WCS matrix, we just need compute f_2', f_3',....., f_{N-2}', f_{N-1}'.

3.3.2 Error Analysis

$$f_1 + \frac{140}{363} f_1' - \frac{1}{h}\left(\frac{980}{363} f_2 - \frac{490}{121} f_3 + \frac{4900}{1089} f_4 - \frac{1225}{363} f_5 + \frac{196}{121} f_6 - \frac{490}{1089} f_7 + \frac{20}{363} f_8\right)$$
$$\sim -\frac{35}{726} f_1^{(8)} h^7$$

$$f_1 + \frac{280}{481} f_1' - \frac{1}{h}\left(\frac{3920}{481} f_3 - \frac{31360}{1443} f_4 + \frac{14700}{481} f_5 - \frac{12544}{481} f_6 + \frac{19600}{1443} f_7 - \frac{1920}{481} f_8 + \frac{245}{481} f_9\right)$$
$$\sim -\frac{280}{481} f_1^{(8)} h^7$$

The combination error in the final weighted compact scheme will be seventh order.

3.4 Boundary Node 2 in Second & Third Boundary Condition

As showing in the previous session, we found f_1 and f_1'. In this session, we are going to focus Node 2 in Second & Third Boundary Condition.

The compact scheme is:

F_0:

$$f_2'+\frac{5}{2}f_3'=\frac{1}{h}(-\frac{1}{12}f_1-\frac{137}{60}f_2+\frac{25}{24}f_3+\frac{5}{3}f_4-\frac{5}{12}f_5+\frac{1}{12}f_6-\frac{1}{120}f_7)$$

F_1:

$$f_2'+6f_3'=\frac{1}{h}(-\frac{69}{20}f_2-\frac{17}{10}f_3+\frac{15}{2}f_4-\frac{10}{3}f_5+\frac{5}{4}f_6-\frac{3}{10}f_7+\frac{1}{30}f_8)$$

F_2:

$$f_2'-\frac{363}{20}f_3'=\frac{1}{h}(\frac{13327}{400}f_3-\frac{1299}{20}f_4+\frac{1369}{24}f_5-39f_6+\frac{285}{16}f_7-\frac{1439}{300}f_8+\frac{23}{40}f_9) \qquad (3.5)$$

Definition of C_k and ω_k is same as (2.6)

$$\omega_k=\frac{\gamma_k}{\sum_{i=0}^{2}\gamma_i} \qquad \gamma_k=\frac{C_k}{(\varepsilon+IS_k)^P} \qquad k=0,1,2$$

3.4.2 Error Analysis

F_0:

$$f_2'+\frac{5}{2}f_3'=\frac{1}{h}(-\frac{1}{12}f_1-\frac{137}{60}f_2+\frac{25}{24}f_3+\frac{5}{3}f_4-\frac{5}{12}f_5+\frac{1}{12}f_6-\frac{1}{120}f_7)\sim\frac{1}{336}f_2^{(8)}h^7$$

F_1:

$$f_2'+6f_3'=\frac{1}{h}(-\frac{69}{20}f_2-\frac{17}{10}f_3+\frac{15}{2}f_4-\frac{10}{3}f_5+\frac{5}{4}f_6-\frac{3}{10}f_7+\frac{1}{30}f_8)\sim-\frac{1}{56}f_2^{(8)}h^7$$

F_2:

$$f_2' - \frac{363}{20} f_3' = \frac{1}{h}\left(\frac{13327}{400} f_3 - \frac{1299}{20} f_4 + \frac{1369}{24} f_5 - 39 f_6 + \frac{285}{16} f_7 - \frac{1439}{300} f_8 + \frac{23}{40} f_9\right)$$

$$\sim -\frac{503}{1120} f_2^{(8)} h^7$$

The combination error in the final weighted compact scheme will be seventh order.

3.5 Matlab Program Code for 2nd & 3rd Boundary Condition

Comply with Matlab syntax, comment line start with %

```
function WCS
% n the number of subintervals
n=40;
h=2*pi/n;
t=linspace(-pi,pi,n+1);
%Test f(x)=sinx
f=sin(t);
%A(:,1) and B(1)is the mixed boundary condition coefficient
%A(1,1)*f(1)+A(1,2)*f'(1)=B(1)
A(1,1)=1;A(1,2)=0;B(1)=0;
A(2,1)=2283;A(2,2)=840*h;
B(2)=6720*f(2)-11760*f(3)+15680*f(4)-14700*f(5)+9408*f(6)-3920*f(7)+960*f(8)-105*f(9);
% Solve the f1 and f1' linear system
x=A\B';
f(1)=x(1);
% Directly copy f1' to the final results
d(1)=x(2);
```

```
%Node N, the same with Node 1
A(1,1)=1;A(1,2)=0;B(1)=0;
A(2,1)=2283;A(2,2)=-840*h;
B(2)=6720*f(n)-11760*f(n-1)+15680*f(n-2)-14700*f(n-3)+9408*f(n-4)-3920*f(n-5)+960*f(n-6)-
105*f(n-7);
% Solve the f_N and f_N' linear system
x=A\B';
f(n+1)=x(1);
% Directly copy f_N' to the final results
d(n+1)=x(2);
H(1)=0;
%Construct H
for i=2:n+2
   H(i)=H(i-1)+f(i-1)*h;
End
% ε = 10^-6
yita =10^-6;
% IS_K
is(1)=13*(f(1)-2*f(2)+f(3))^2/12+(f(1)-4*f(2)+3*f(3))^2/4;
is(2)=13*(f(2)-2*f(3)+f(4))^2/12+(f(2)-f(4))^2/4;
is(3)=13*(f(3)-2*f(4)+f(5))^2/12+(3*f(5)-4*f(4)+f(3))^2/4;
 % γ_K
gama(1)=1/(yita+is(1));
gama(2)=1/(yita+is(2));
gama(3)=1/(yita+is(3));
s=sum(gama);
```

```
% ω_k
for i=1:3
w(i)=gama(i)/s;
end
% Right hand side of F_k
fr(1)=-10*H(1)-274*H(2)+125*H(3)+200*H(4)-50*H(5)+10*H(6)-H(7);
fr(2)=-207*H(2)-102*H(3)+450*H(4)-200*H(5)+75*H(6)-18*H(7)+2*H(8);
fr(3)=39981*H(3)-77940*H(4)+68450*H(5)-46800*H(6)+21375*H(7)-5756*H(8)+690*H(9);
% Left hand side of F_k , A(1,1) is f_1',A(1,2) is f_2',A is defined as WCS main matrix
A(1,1)=120*w(1)+60*w(2)+1200*w(3);
A(1,2)=300*w(1)+360*w(2)-21780*w(3);
% Right hand side of F
B(1)=(w(1)*fr(1)+w(2)*fr(2)+w(3)*fr(3))/h;
for j=3:n-1
clear gama;
is(1)=13*(f(j-2)-2*f(j-1)+f(j))^2/12+(f(j-2)-4*f(j-1)+3*f(j))^2/4;
is(2)=13*(f(j-1)-2*f(j)+f(j+1))^2/12+(f(j-1)-f(j+1))^2/4;
is(3)=13*(f(j)-2*f(j+1)+f(j+2))^2/12+(3*f(j)-4*f(j+1)+f(j+2))^2/4;
 gama(1)=1/(18*(yita+is(1))^0.5);
 gama(2)=8/(9*(yita+is(2))^0.5);
 gama(3)=1/(18*(yita+is(3))^0.5);
s=sum(gama);
for i=1:3
w(i)=gama(i)/s;
end
A(j-1,j-2)=2*w(1)+w(2)/4;
```

```
A(j-1,j-1)=1;
A(j-1,j)=2*w(3)+w(2)/4;
B(j-1)=(-1*w(1)*H(j-2)/2+(-2*w(1)-3*w(2)/4)*H(j-1)+(5*w(1)/2-
5*w(3)/2)*H(j)+(2*w(3)+3*w(2)/4)*H(j+1)+w(3)*H(j+2)/2)/h;
end
clear gama;
is(3)=13*(f(n+1)-2*f(n)+f(n-1))^2/12+(f(n+1)-4*f(n)+3*f(n-1))^2/4;
is(2)=13*(f(n)-2*f(n-1)+f(n-2))^2/12+(f(n)-f(n-2))^2/4;
is(1)=13*(f(n-1)-2*f(n-2)+f(n-3))^2/12+(3*f(n-1)-4*f(n-2)+f(n-3))^2/4;
gama(1)=1/(18*(yita+is(1))^0.5);
gama(2)=8/(9*(yita+is(2))^0.5);
gama(3)=1/(18*(yita+is(3))^0.5);
s=sum(gama);
for i=1:3
w(i)=gama(i)/s;
end
A(n-1,n-2)=2*w(1)+w(2)/4;
A(n-1,n-1)=1;
A(n-1,n)=2*w(3)+w(2)/4;
B(n-1)=(-1*w(1)*H(n-2)/2+(-2*w(1)-3*w(2)/4)*H(n-1)+(5*w(1)/2-
5*w(3)/2)*H(n)+(2*w(3)+3*w(2)/4)*H(n+1)+w(3)*H(n+2)/2)/h;
clear gama;
gama(1)=1/(yita+is(1));
gama(2)=1/(yita+is(2));
gama(3)=1/(yita+is(3));
s=sum(gama);
```

```
for i=1:3
w(i)=gama(i)/s;
end
fr(1)=10*H(n+2)+274*H(n+1)-125*H(n)-200*H(n-1)+50*H(n-2)-10*H(n-3)+H(n-4);
fr(2)=207*H(n+1)+102*H(n)-450*H(n-1)+200*H(n-2)-75*H(n-3)+18*H(n-4)-2*H(n-5);
fr(3)=-39981*H(n)+77940*H(n-1)-68450*H(n-2)+46800*H(n-3)-21375*H(n-4)+5756*H(n-5)-
690*H(n-6);
A(n,n)=120*w(1)+60*w(2)+1200*w(3);
A(n,n-1)=300*w(1)+360*w(2)-21780*w(3);
B(n)=(w(1)*fr(1)+w(2)*fr(2)+w(3)*fr(3))/h;
% Solve the main WCS matrix to compute H'
x=A\B';
% Transfer H' to f'
for i=1:n-1
   d(i+1)=(x(i+1)-x(i))/h;
end
% plot error
plot(t,d-cos(t))
```

CHAPTER 4

NUMERICAL RESULTS

In this chapter, the sixth-order WCS derived in the previous chapter will be used to test sine function, exponential function, and analyze the numerical error.

4.1 $f(x) = sinx$

We are going to test $f(x) = sinx$, and of course $f' = cosx$.

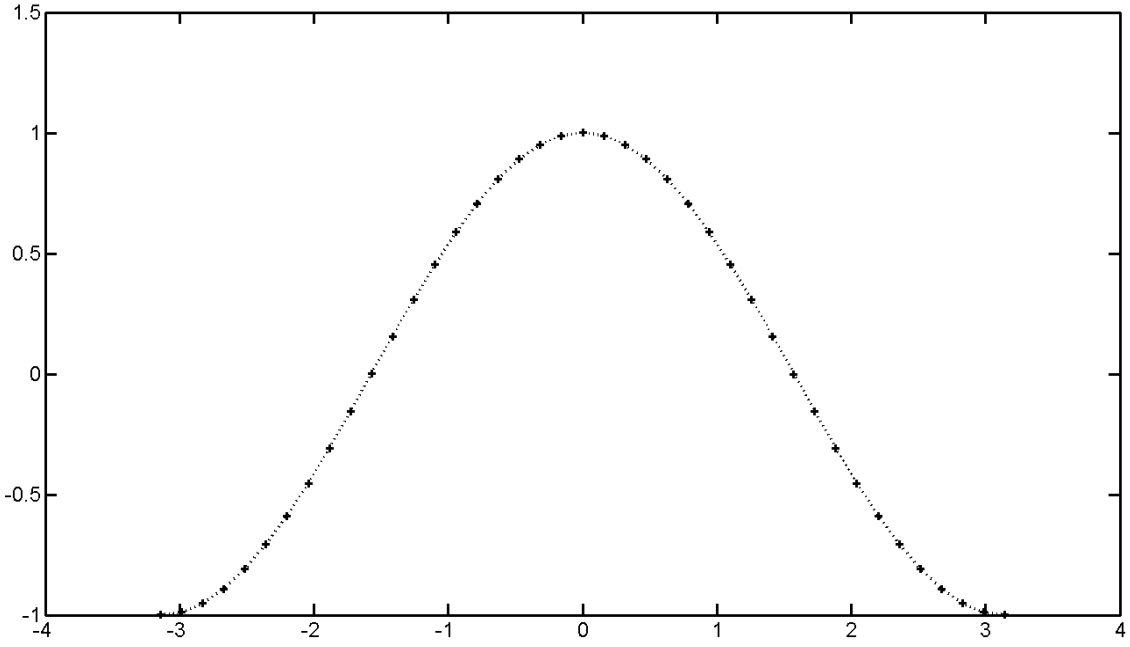

Figure 4.1 $f(x) = sinx$ $\quad -\pi \le x \le \pi$ Subinterval 40

+ WCS numerical results …exact results

The following diagram is the sixth-order WCS numerical error:

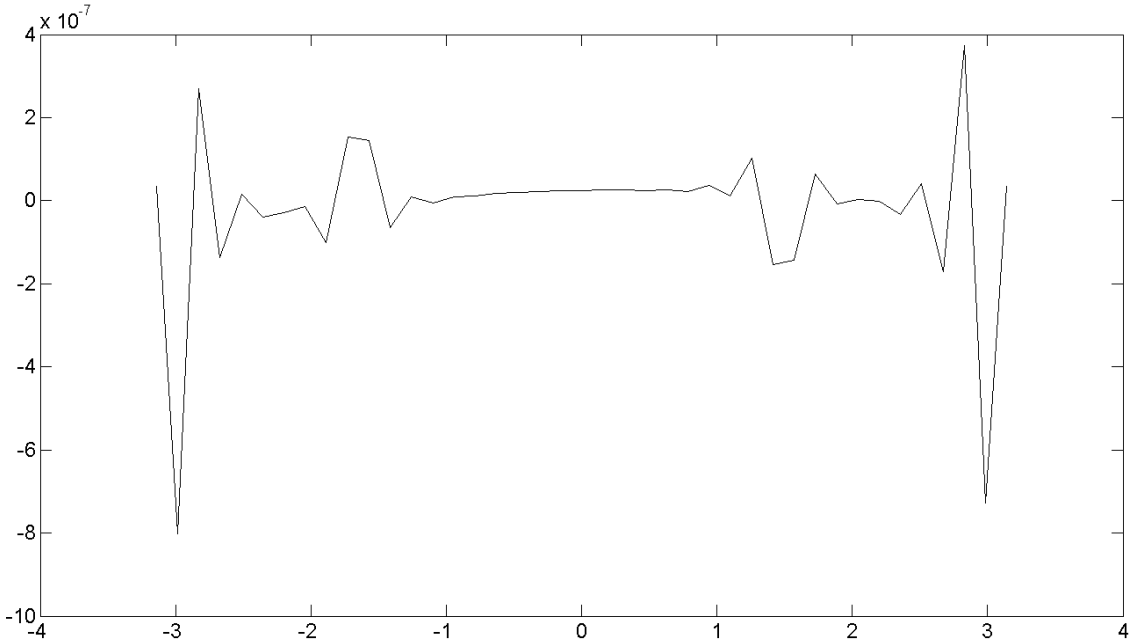

Figure 4.2 $f(x) = sinx \qquad -\pi \leq x \leq \pi$ Subinterval 40

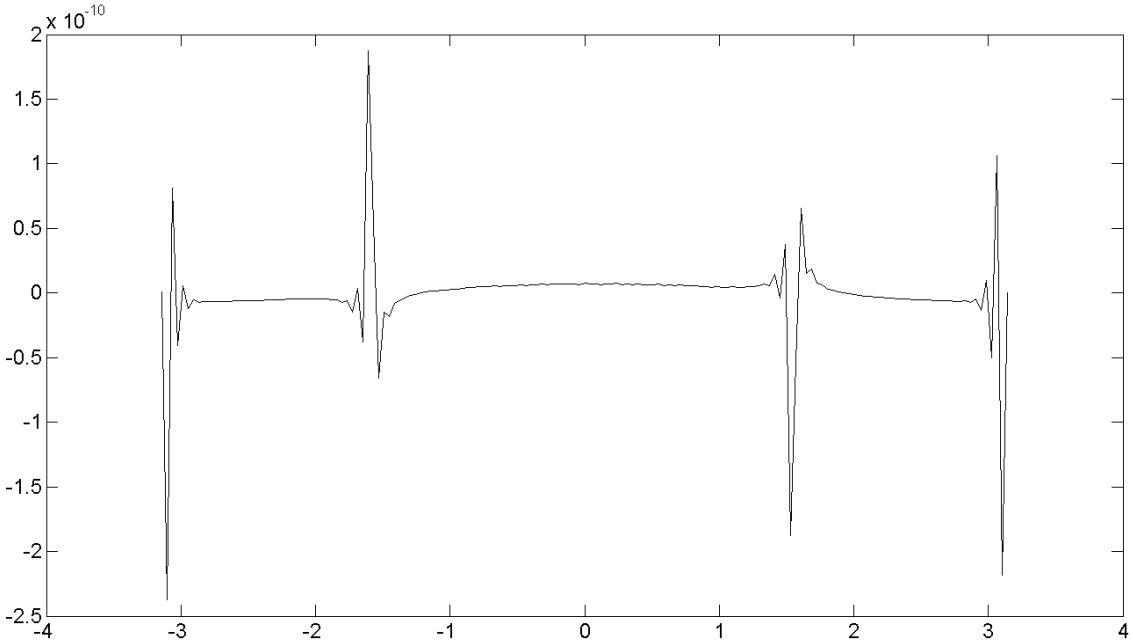

Figure 4.3 $f(x) = sinx \qquad -\pi \leq x \leq \pi$ Subinterval 160

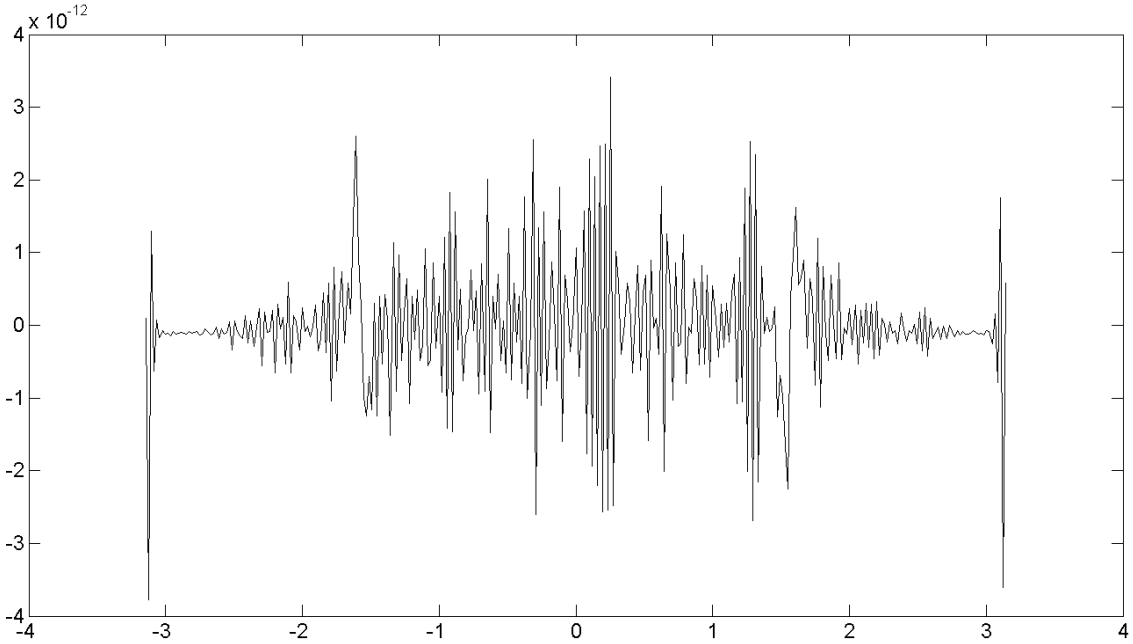

Figure 4.4 $f(x) = sinx \qquad -\pi \le x \le \pi$ Subinterval 320

4.1.2 Accuracy Order Analysis

Table 4.1 Accuracy Order $f(x) = sinx$

Subinterval	L_1 Error	Order	L_2 Error	Order	L_∞ Error	Order
20	0.001512		0.000999		0.000706	
40	4.47E-05	5.0806	2.89E-05	5.11276	2.04E-05	5.1133
80	8.15E-07	5.77634	5.09E-07	5.82463	3.6E-07	5.82495
160	1.38E-08	5.88296	8.2E-09	5.95768	5.79E-09	5.95819
320	3.85E-10	5.16506	1.31E-10	5.96845	9.23E-11	5.97018

The order analysis shows explicitly, the Weighted Compact Boundary Scheme can guarantee the global WCS are sixth-order accuracy.

4.2 Exponential function $f(x) = exp(-300x^2)$

$f(x) = exp(-300x^2)$, then $f'(x) = -600exp(-300x^2)$. We are going to test the new Weighted Compact Boundary Scheme by $f(x) = exp(-300x^2)$

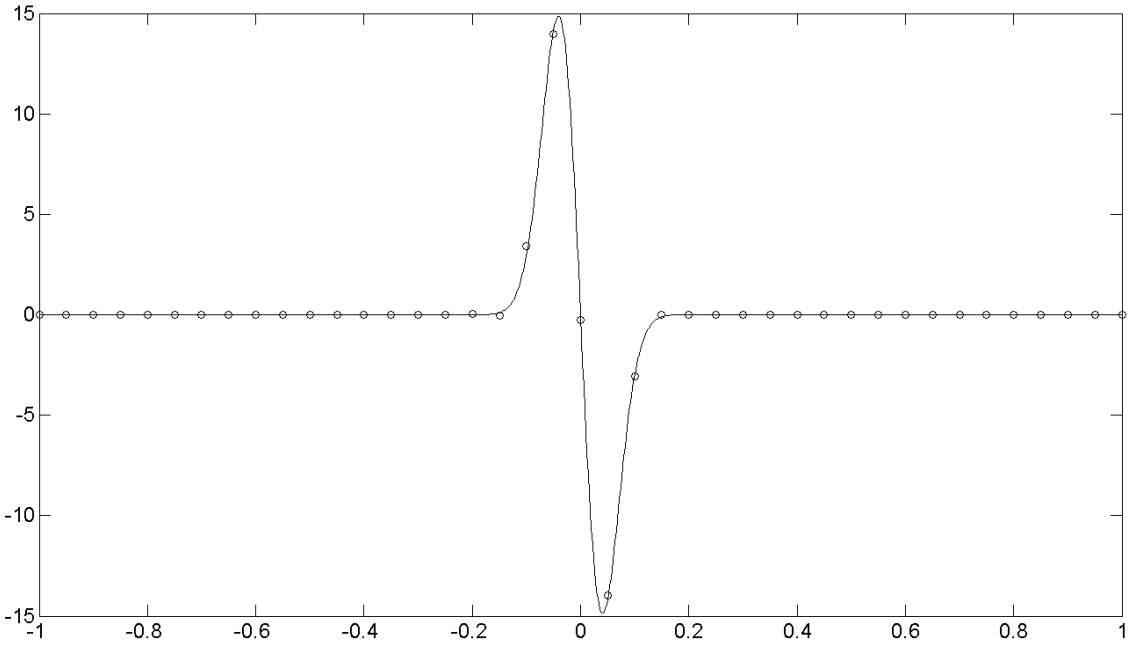

Figure 4.5 $f(x) = exp(-300x^2)$ $-1 \le x \le 1$ Subinterval 40

o WCS numerical results - exact results

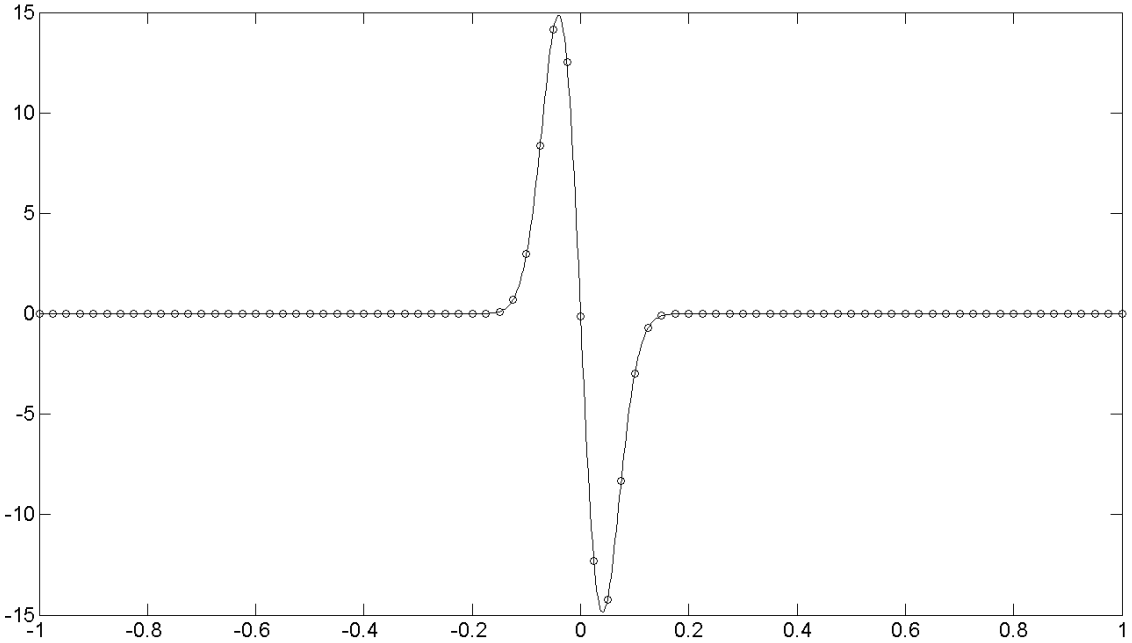

Figure 4.6 $f(x) = exp(-300x^2)$ $-1 \le x \le 1$ Subinterval 80

o WCS numerical results - exact results

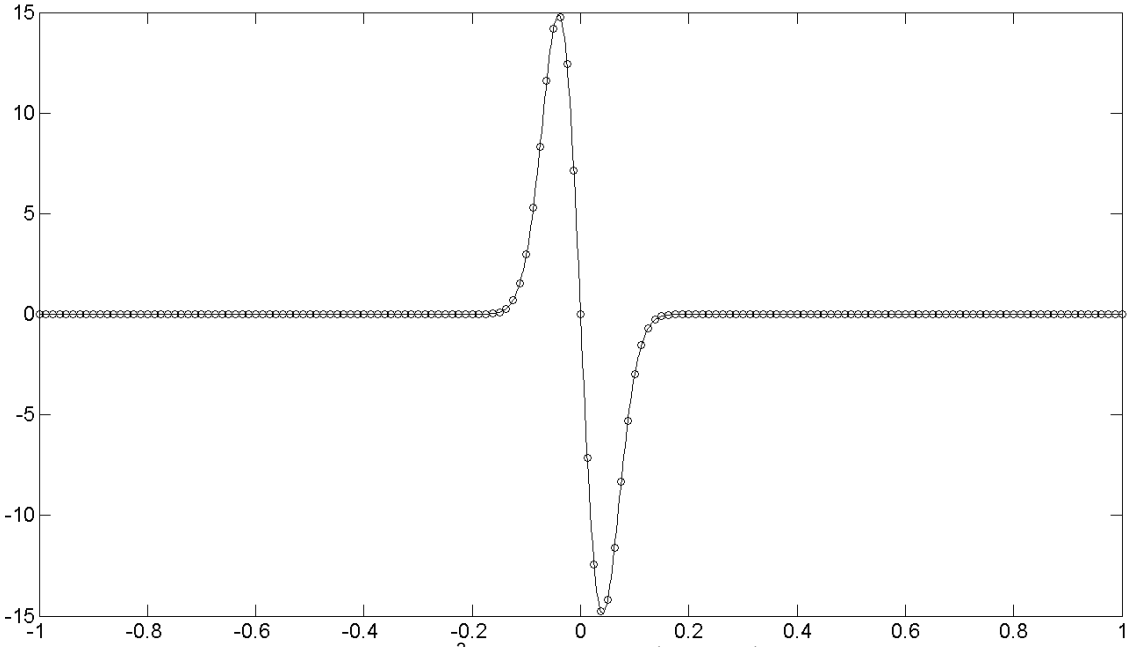

Figure 4.7 $f(x) = exp(-300x^2)$ $-1 \le x \le 1$ Subinterval 160

o WCS numerical results - exact results

4.2.2 Error Analysis

Table 4.2 Accuracy Order $f(x) = exp(-300x^2)$

Subinterval	L_1 Error	Order	L_2 Error	Order	L_∞ Error	Order
20	12.13257		6.622628		5.498617	
40	1.51641	3.00015	0.617534	3.42281	0.424323	3.69583
80	0.547779	1.46899	0.220403	1.48638	0.139669	1.60315
160	0.011333	5.59505	0.003176	6.11701	0.002358	5.88829
320	0.000287	5.30396	5.61E-05	5.82311	3.51E-05	6.06804

The order analysis shows explicitly, the Weighted Compact Boundary Scheme can guarantee the global WCS are sixth-order accuracy.

4.3 Exponential function $f(x) = exp(-300(x+0.959)^2)$

This numerical test of exponential function $f(x) = exp(-300(x+0.959)^2)$ is focus on the ability of Weighted Compact Boundary Scheme. Because $f(x) = exp(-300(x+0.959)^2)$ has a severely deep slop at boundary $x = -1$. And we are going to test 2nd Boundary condition. That is $f'(-1) = -600(-1+0.959)\exp(-300(-1+0.959)^2)$. The numerical results are followed: $f(x) = exp(-300(x+0.959)^2)$, then $f' = -600(x+0.959)\exp(-300(x+0.959)^2)$.

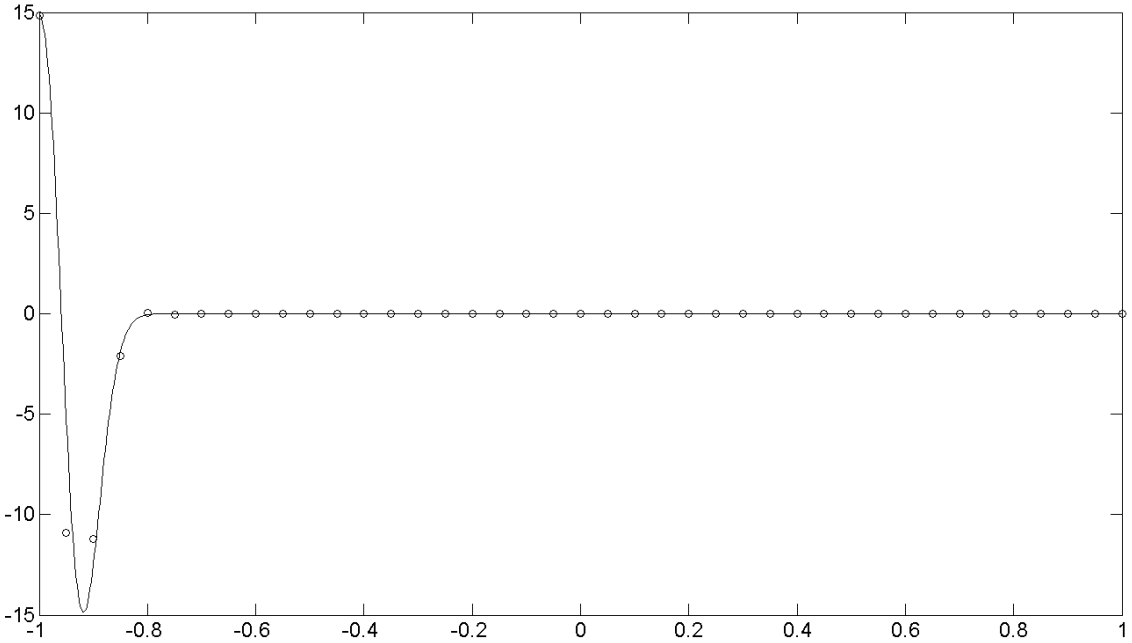

Figure 4.8 WCS $f(x) = exp(-300(x+0.959)^2)$ $-1 \le x \le 1$ Subinterval 40

o WCS numerical results - exact results

Comparing with Compact Scheme of 40 subintervals

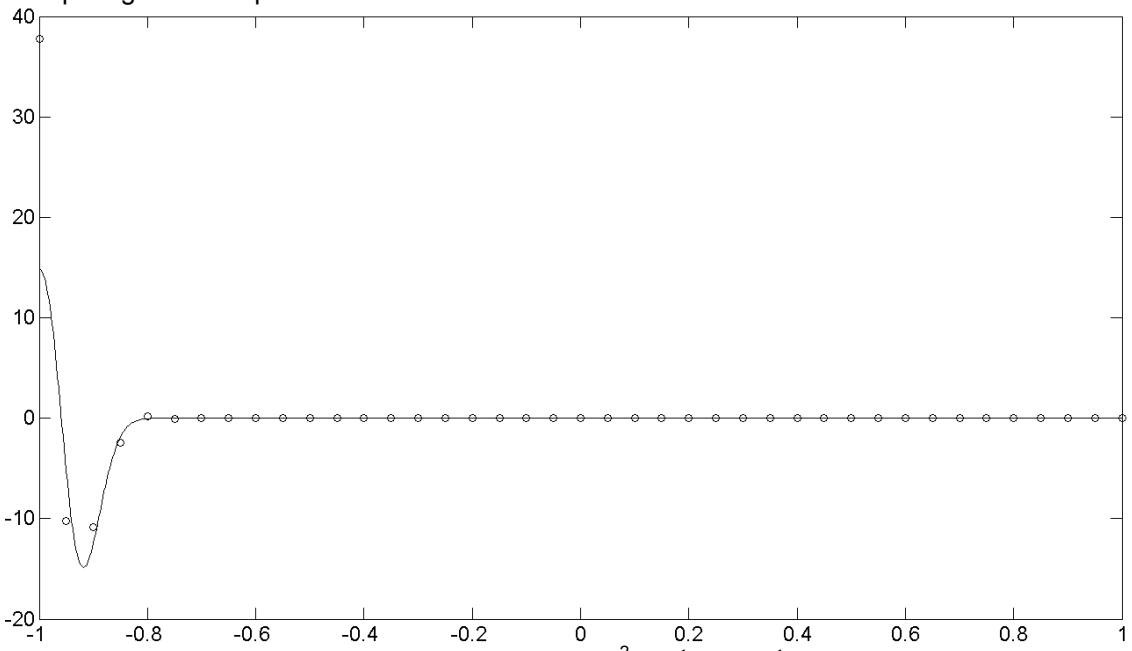

Figure 4.9 CS $f(x) = exp(-300(x+0.959)^2)$ $-1 \le x \le 1$ Subinterval 40

o CS numerical results - exact results

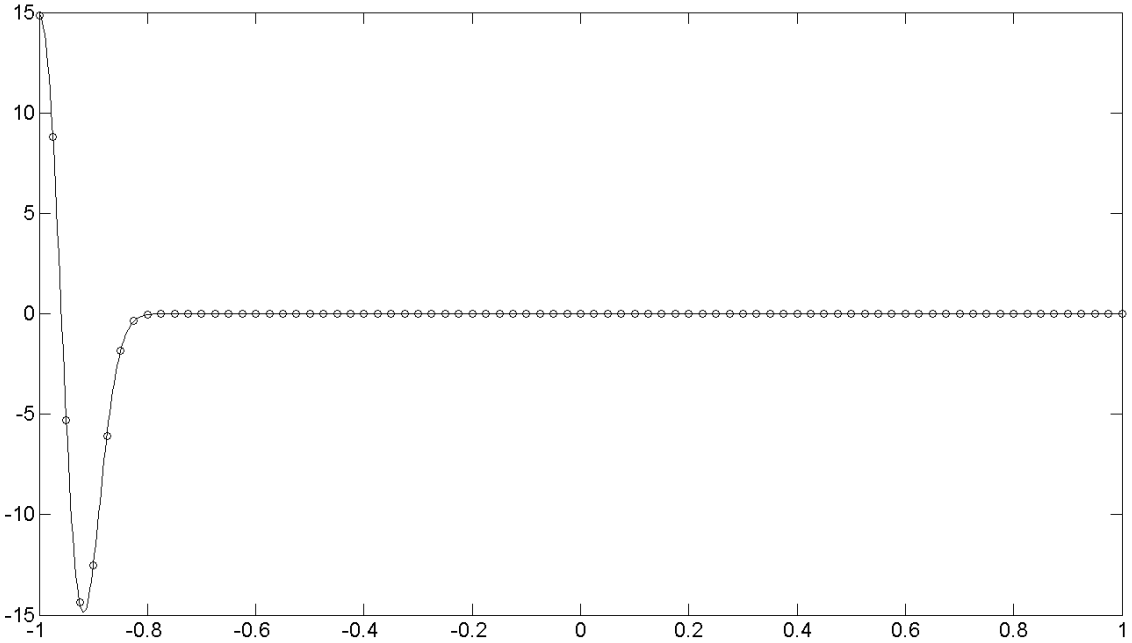

Figure 4.10 WCS $f(x) = exp(-300(x+0.959)^2)$ $-1 \le x \le 1$ Subinterval 80

o WCS numerical results - exact results

Comparing with Compact Scheme of 80 subintervals

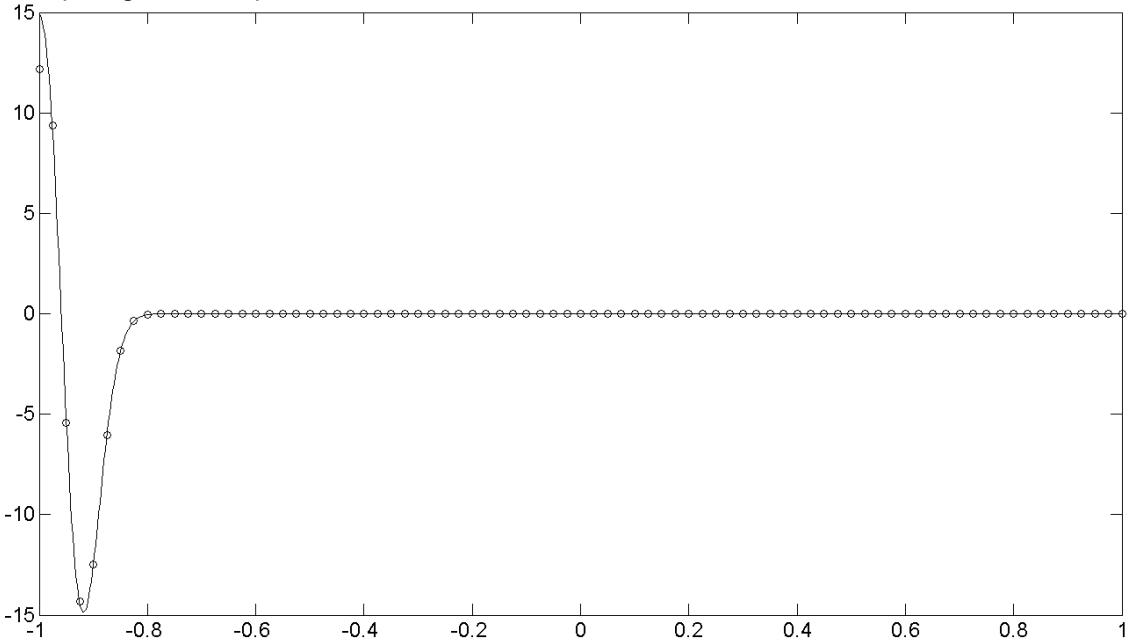

Figure 4.11 CS $f(x) = exp(-300(x+0.959)^2)$ $-1 \le x \le 1$ Subinterval 80

o CS numerical results - exact results

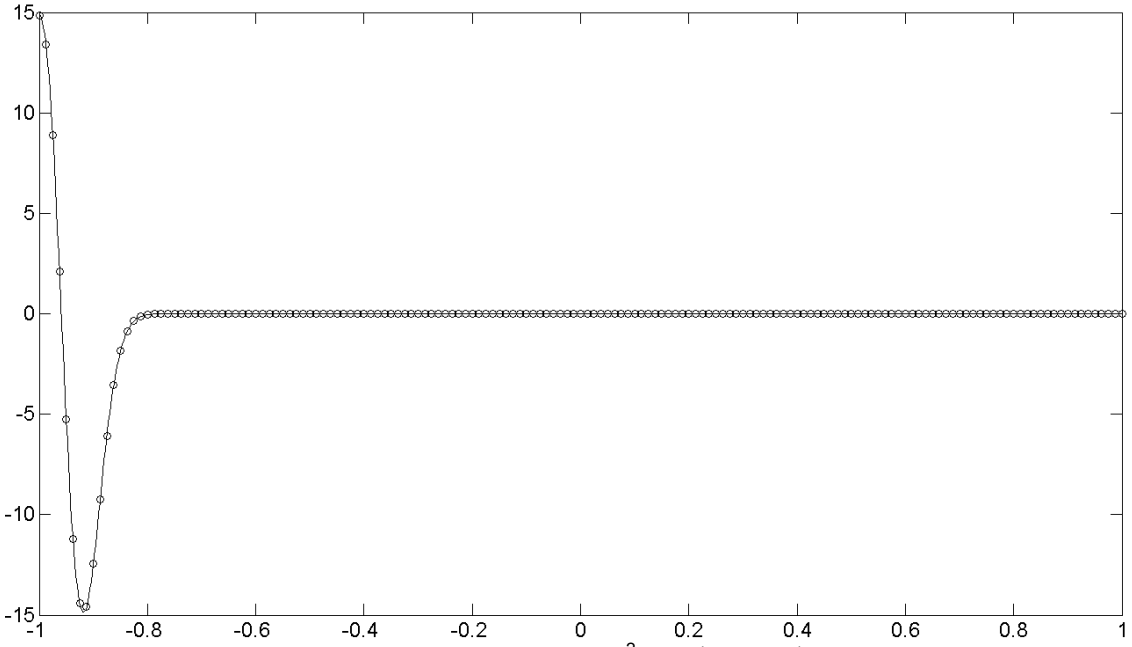

Figure 4.12 WCS $f(x) = exp(-300(x+0.959)^2)$ $-1 \le x \le 1$ Subinterval 160

o WCS numerical results - exact results

Comparing with Compact Scheme of 160 subintervals

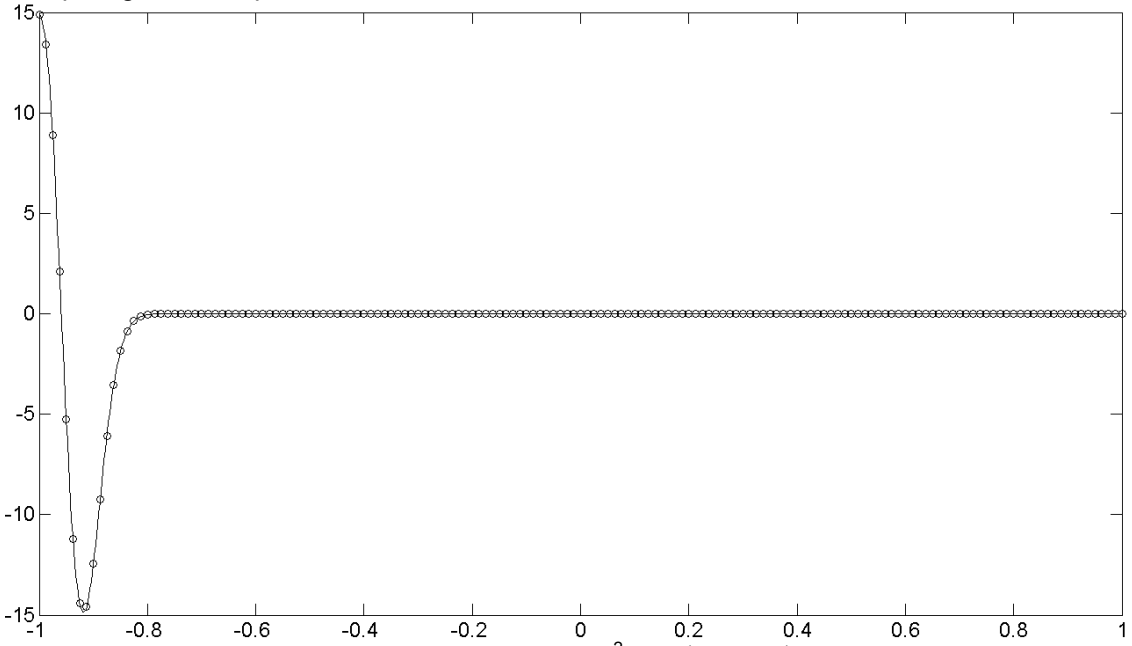

Figure 4.13 CS $f(x) = exp(-300(x+0.959)^2)$ $-1 \le x \le 1$ Subinterval 160

o CS numerical results - exact results

The numerical results showed that this Weighted Compact Boundary Scheme can precisely capture the deep slop at the neighborhood of left boundary. And the ability of capturing is much better than Compact Scheme at the boundary.

4.4 Exponential function $f(x) = exp(-300(x-0.959)^2)$

In this session, we are going to test the Weight Compact Boundary Scheme under the 3rd Boundary Condition

$$f(x) + f'(x) = \exp(-300(x-0.959)^2) - 600(x-0.959)\exp(-300(x-0.959)^2) \qquad x=1.$$

The results comparing to Compact Scheme at the boundary will show a much better capturing ability.

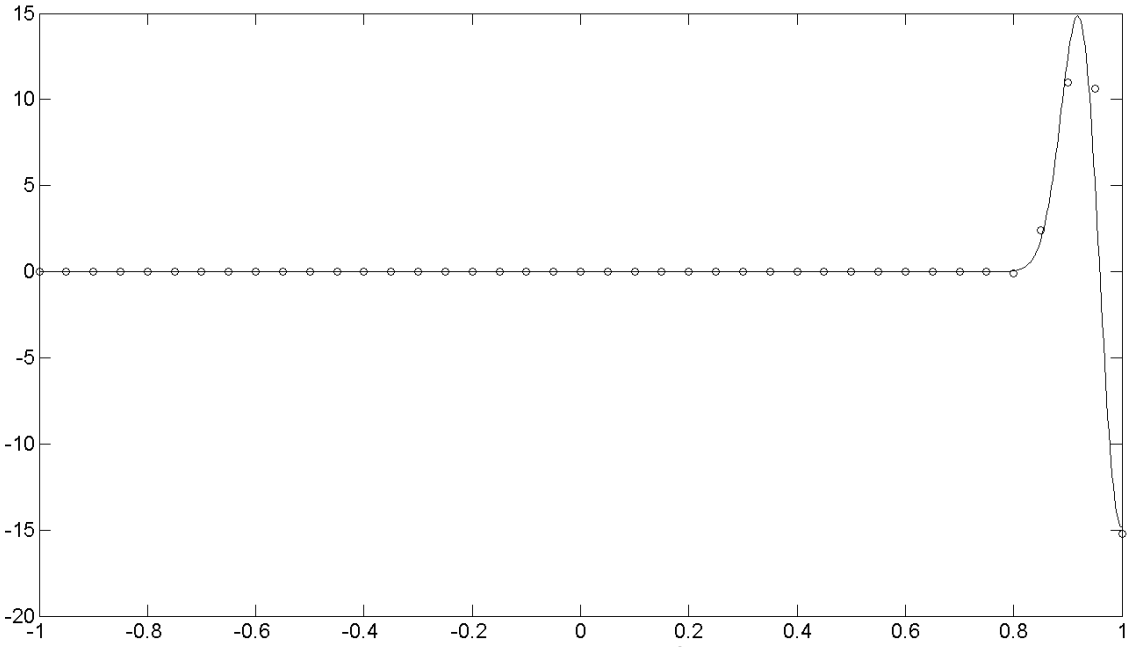

Figure 4.14 WCS $f(x) = \exp(-300(x-0.959)^2) \quad -1 \le x \le 1$ Subinterval 40

o WCS numerical results - exact results

Comparing Compact Scheme with 40 subintervals:

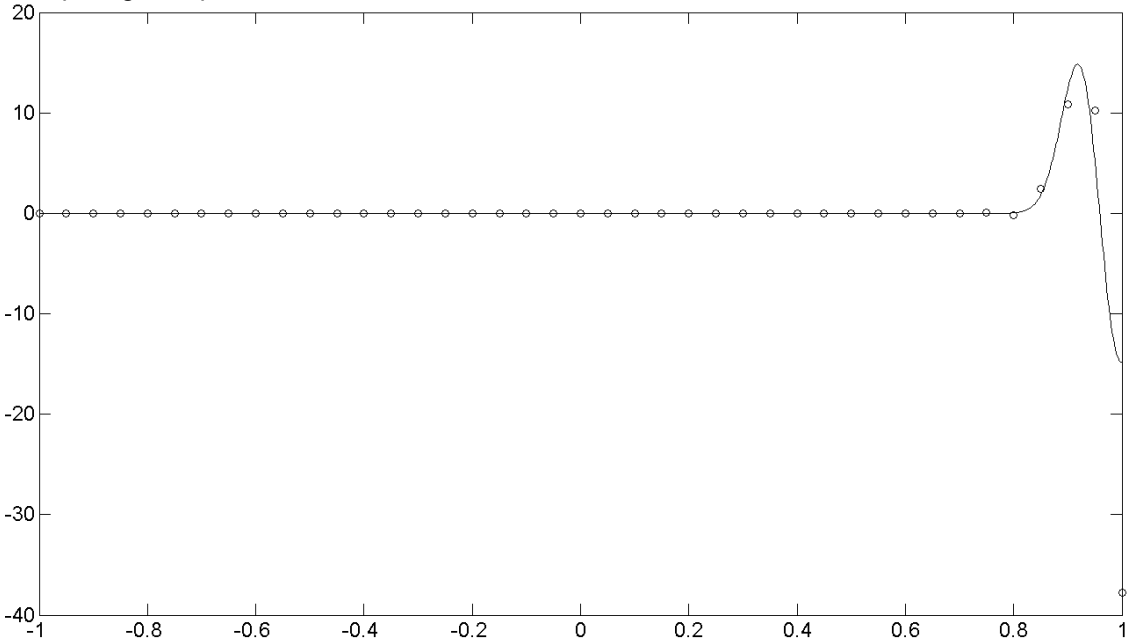

Figure 4.15 CS $f(x) = \exp(-300(x-0.959)^2) \quad -1 \le x \le 1$ Subinterval 40

o CS numerical results - exact results

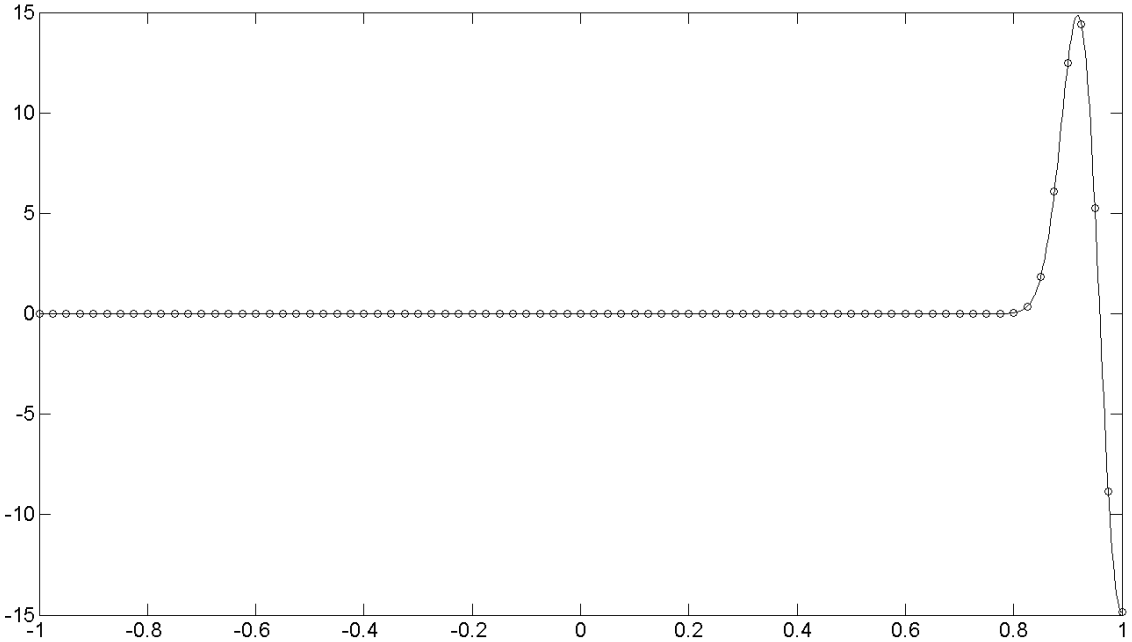

Figure 4.16 WCS $f(x) = \exp(-300(x-0.959)^2) \quad -1 \le x \le 1$ Subinterval 80

o WCS numerical results - exact results

Comparing Compact Scheme with 80 subintervals:

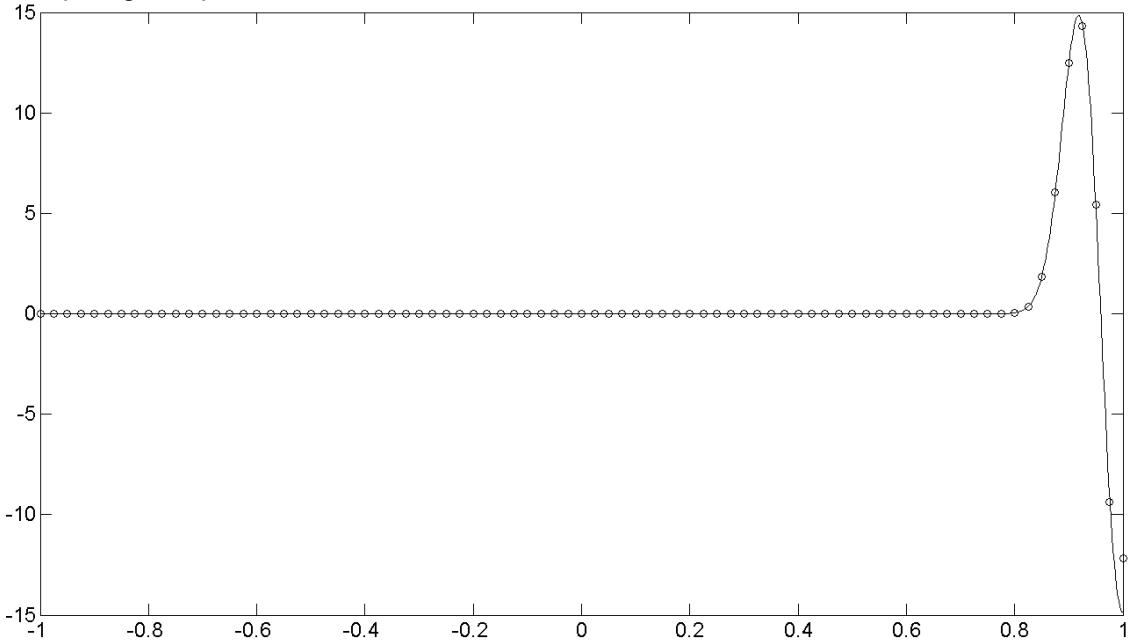

Figure 4.17 CS $f(x) = \exp(-300(x-0.959)^2) \quad -1 \le x \le 1$ Subinterval 80

o CS numerical results - exact results

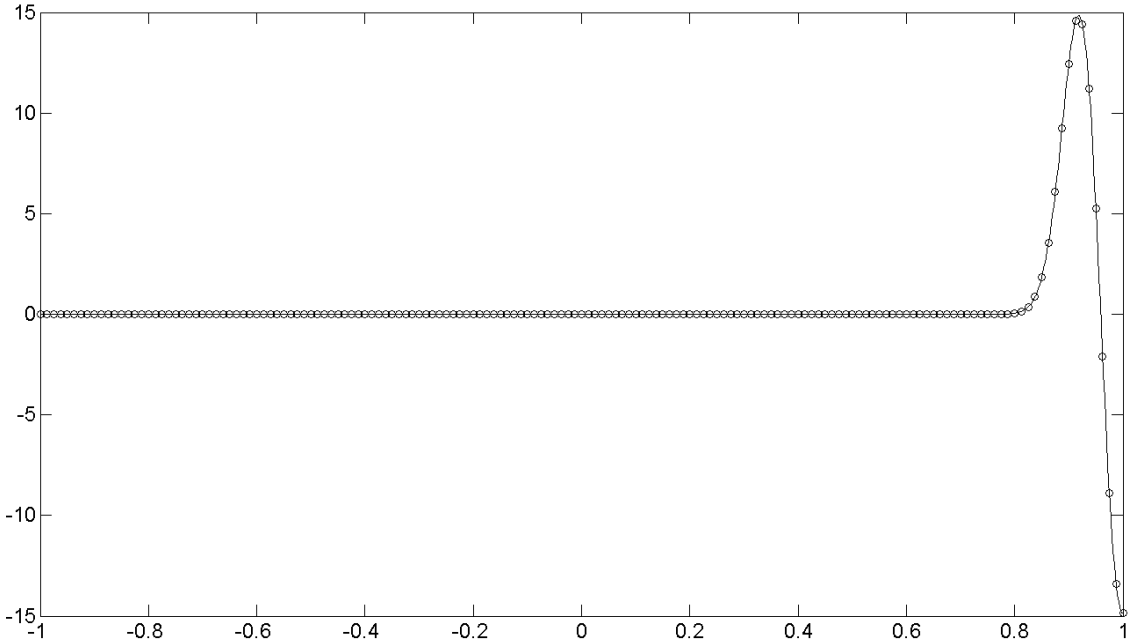

Figure 4.18 WCS $f(x) = \exp(-300(x-0.959)^2) \quad -1 \le x \le 1$ Subinterval 160

o WCS numerical results - exact results

Comparing Compact Scheme with 160 subintervals:

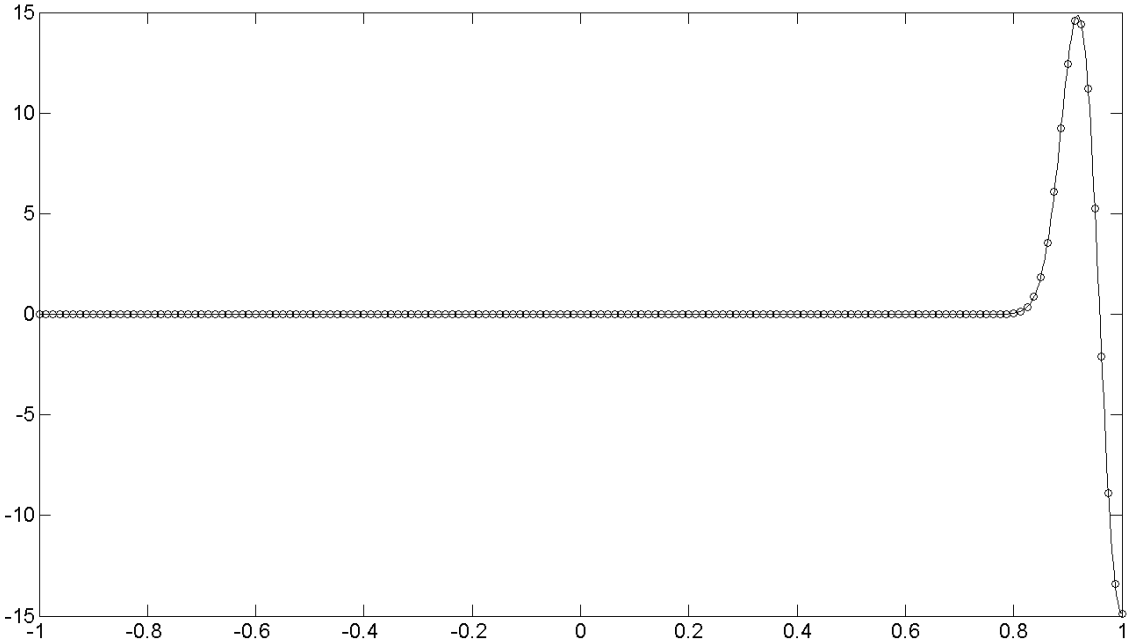

Figure 4.19 CS $f(x) = \exp(-300(x-0.959)^2) \quad -1 \le x \le 1$ Subinterval 160

o CS numerical results - exact results

CHAPTER 5

CONCLUSIONS AND FUTURE WORK

The Weighted Compact boundary conditions developed in this work has been successfully tested. This Weighted Compact boundary conditions derived have shown to achieve higher order accuracy and high resolution. So the basic work of deriving the equations for one dimension has been successfully done in this paper.

The future work would involve applying the WCS for multi-dimension flows, DNS/LES and flows with shock-turbulence interactions. Before we do this, we have one more issue is that test the interaction of shocks and discontinuities at the boundaries. In all our present problems tested, we have not encountered shock interaction with the boundaries. Hence the future work is very challenging, interesting and promising.

REFERENCES

[1] L. Jiang, H. Shan and C. Liu Weighted Compact Scheme for Shock Capturing. *IJCFD*, 2001, Vol. 15, pp. 147-155

[2] A. Harten, B. Engquist, S. Osher and Chakravarthy(1987). Uniformly high order accurate essentially non-oscillatory scheme, III, *JCP*, 71, 231-303.

[3] S. K. Lele(1992) Compact finite difference schemes with spectral-like resolution, *JCP*, 103, 16-42

[4] X. D. Liu, S. Osher, and T. Chan, (1994) Weighted Essential Non-Oscillatory Schemes, *JCP*, 115,200-212.

[5] G. S. Jiang and C. W Shu (1996) Efficient Implementation of Weighted ENO Scheme, *JCP*, 126,202-228

[6] M. R. Visbal and D. Gaitonde (1998) High-Order Accurate Methods for Unsteady Vertical Flows on Curvilinear Meshes, *AIAA paper* 98-0131.

[7] Amith Madhav Kalaghatagi, Higher Order Compact Boundary Conditions For Weighted Compact Scheme, UT Arlington, *UMI* 1418174

[8] S. F. Davis (1998) Shock Capturing with Pade Methods, Applied Mathematics and Computation 89:85-89

[9] C. W. Shu and S. Osher (1988), Efficient Implementation of Essentially Non-Oscillatory Shock Capturing Schemes, *JCP*, 77, 439-471.

[10] C. W. Shu and S. Osher (1989) Efficient Implementation of Essentially Non-Oscillatory Shock Capturing Shemes II, *JCP*, 83, 32-78.

[11] C. W. Shu (1999) High Order ENO and WENO Schemes for Computational Fluid Dynamics, Higher Order Methods for Computational Physics, *Springer*, 9, 439-582.

[12] A. Harten and S. Osher (1987) Uniformly High-Order Accurate Non-Oscillatory Schemes, I, *SIAM Journal on Numerical Analysis,* v24, 279-309.

[13] N. A. Adams and K. Shariff (1996) A High-Resolution Hybrid Compact-ENO Scheme for Shock-Turbulence Interaction Problems, *JCP*, 127, 27-51.

BIOGRAPHICAL INFORMATION

Mr. Zhengjie Wang's research interests broadly are Ocean Engineering, Naval Architecture, Experimental Fluid Dynamics, Computational Fluid Dynamics and Applied Mathematics. So far, his course work and research work has been focused on the listed areas. In the Master study and this thesis, he presented more sophisticated coding techniques. In Numerical Analysis, writing codes of course is the necessary skill. And Mr. Wang showed the ability to manipulate these techniques to various mathematical, numerical projects and practical engineering problems. It was very challenging, interesting and a unique leaning experience for him to develop the Weighted Compact boundary conditions for the Weighted Compact Scheme.

After graduating with his Master, he wants to magnify all these Marine Structure, Fluid, and Applied Mathematics technology charm to scientific research and engineering. And after gained more scientific engineering experience, he would like to pursue for a doctoral degree in the future.